



Effects of the composition on the properties of nickel–aluminum layered double hydroxide/carbon (Ni–Al LDH/C) composite fabricated by liquid phase deposition (LPD)

Alexis Bienvenu Béléké^{a,1}, Eiji Higuchi^b, Hiroshi Inoue^b, Minoru Mizuhata^{a,*}

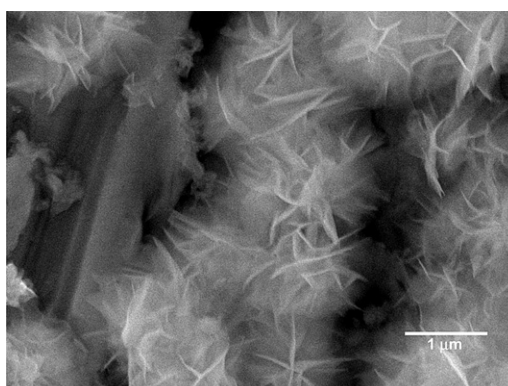
^a Department of Chemical Science and Engineering, Graduate School of Engineering, Kobe University, 1-1 Rokkodai-cho, Nada, Kobe 657-8501, Japan

^b Department of Applied Chemistry, Graduate School of Engineering, Osaka Prefecture University, 1-1 Gakuen-cho, Nakaku Sakai, Osaka 599-8531, Japan

HIGHLIGHTS

- We report the optimized preparation of Ni–Al LDH/C composite by the LPD method.
- We investigate the influence of the LDH content on the properties of the composite.
- The crystallinity of the composite increases with increasing the LDH content.
- The optimized composition results in high performance cathode materials.
- The electrode displays high discharge capacity, good cycle life and excellent electrochemical stability.

GRAPHICAL ABSTRACT



ARTICLE INFO

Article history:

Received 23 September 2012

Accepted 12 October 2012

Available online 23 October 2012

Keywords:

Layered double hydroxide
Active materials
Electrode
Ni–MH batteries

ABSTRACT

We report the optimized preparation by liquid phase deposition (LPD) of nickel–aluminum layered double hydroxide/carbon (Ni–Al LDH/C) composites as nickel-based cathode materials. We investigate the influence of the LDH content on the properties of the composites prepared with various total volumes of the reaction solution while the solution composition and the amount of carbon are maintained constant. Diffraction patterns show that the crystallinity of the composite increases with increasing the LDH content. Gravimetric studies indicate that there is no correlation between the amount of the deposit and the total volume of the reaction solution. Inductively coupled plasma-atomic emission spectroscopy (ICP-AES) reveals that the optimal $\text{Al}^{3+}/(\text{Al}^{3+} + \text{Ni}^{2+})$ is obtained for the sample with the highest LDH content. The optimized composition results in high performance cathode materials; a high discharge capacity ($>390 \text{ mAh g}_{\text{comp}}^{-1}$) at the 1.0 C-rate, a good cycle life at 2.0 C-rate over 300 cycles and excellent electrochemical stability.

© 2012 Elsevier B.V. All rights reserved.

1. Introduction

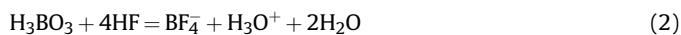
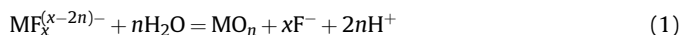
Layered double hydroxide (LDH) materials belong to the family of natural anionic clays with general formula $[\text{M}^{2+}_{1-x}\text{M}^{3+}_x] \text{A}_x/\text{n}^-(\text{OH})_2 \cdot y\text{H}_2\text{O}$ ($\text{A}^{n-} = \text{OH}^-, \text{CO}_3^{2-}, \text{NO}_3^-$) in which the substitution of a certain fraction x of the divalent cations with trivalent ones gives

* Corresponding author. Tel./fax: +81 78 803 6186.

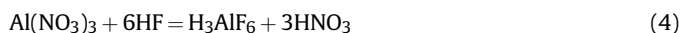
E-mail address: mizuhata@kobe-u.ac.jp (M. Mizuhata).

¹ Present address: Minings and Materials Engineering, McGill University, Wong Bldg, 3610 University St., Montreal, QC H3A 0C5, Canada.

rise to a net positive charge. The excess of positive charge is compensated with anions contained in the interslabs [1,2]. For example, the most popular compound in this category of LDH materials is hydrotalcite, $\text{Mg}_6\text{Al}_2(\text{CO}_3)(\text{OH})_{16} \cdot 4\text{H}_2\text{O}$. Due to their anion exchange properties and capacity to intercalate anions, the LDH materials have potential applications in various fields including catalysis [3], anion exchangers [4,5], precursors to oxides [6], magnetics [7,8], and electrodes for rechargeable alkaline batteries [9,10]. For battery applications, nickel–aluminum LDH (also called Al-substituted α -Ni(OH)₂) appears to be the most promising cathode active material for the next generation of rechargeable alkaline batteries because of its good stability [11–13]. These materials are usually prepared by the common methods such as coprecipitation [14], hydrothermal [15] or electrochemical reactions [11]. Recently, we have employed a novel approach to prepare nickel–aluminum LDH/carbon (Ni–Al LDH/C) composite for battery applications, namely the liquid phase deposition (LPD) method [16,17]. The LPD is one of the *chimie douce* techniques of preparation of metal oxide thin films developed by Nagayama et al. [18], and pioneered by Deki's group for the past two decades [19–21]. Its basic concept is described elsewhere [16–22] and the main reactions can be expressed as follows.



In the conventional LPD process, the metal-fluoro complex is hydrolyzed to form fluoride, Eq. (1), and the fluoride is trapped by boric acid (H_3BO_3), Eq. (2), or aluminum metal Eq. (3) which acts as a fluoride scavenger. In this study, $\text{Al}(\text{NO}_3)_3$, Eq. (4) is used as a raw material to form the Ni–Al LDH as well as a fluoride scavenger. $\text{Al}(\text{NO}_3)_3$ can trap fluoride as follows:



In this context, the LPD offers the possibility to control the amount of Al^{3+} cations substituted in the $\text{Ni}(\text{OH})_2$ lattices, the amount of the resulting films deposited over carbon particles, as well as other advantages such as phase purity, crystallinity and no pH adjustment.

In order to produce high performance devices, it is necessary to optimize the synthetic route. In our previous work, we focused on the optimum range for Al^{3+} substitution (Al ratio). In this paper we concentrate on the amount of Ni–Al LDH deposited on carbon particles, i.e., the LDH content. Both the LDH content and the $\text{Al}^{3+}/(\text{Al}^{3+} + \text{Ni}^{2+})$ seem to be crucial for the electrochemical performance of the Ni–Al LDH/C positive electrodes. The Ni–Al LDH/C composites which had various LDH contents and the $\text{Al}^{3+}/(\text{Al}^{3+} + \text{Ni}^{2+})$ were characterized by X-ray diffractions (XRD), scanning electron microscope (SEM), inductively coupled plasma-atomic emission spectroscopy (ICP-AES). The performance of these cathode materials was evaluated by charge–discharge measurements at 1.0 C-rate. The durability and the electrochemical stability of the Ni–Al LDH/C electrode with the highest LDH content and optimal $\text{Al}^{3+}/(\text{Al}^{3+} + \text{Ni}^{2+})$ were also evaluated.

2. Experimental

2.1. Materials and composite preparation

Carbon black with 50 nm of primary average diameter and 50 m²/g of the specific surface area was used as a conductive agent.

The carbon surface was preheated above 1000 °C and oxidized using KMnO_4 aqueous solution. The materials, the reaction solution, the carbon pretreatment and the synthesis of Ni–Al LDH/C composites were conducted according to the procedure similar to our previous work [16,17]. In a typical procedure, 20 mg of oxidized carbon was put in a plastic polypropylene bottle. Then appropriate amounts of (i) Ni parent aqueous solution (containing 30 mM (=mmol dm^{−3}) Ni^{2+} in 0.66 M NH_4F), (ii) 0.5 M aqueous H_3BO_3 and (iii) 0.05 M aqueous $\text{Al}(\text{NO}_3)_3 \cdot 9\text{H}_2\text{O}$, were mixed and diluted with deionized water to give a reaction solution with final concentrations of Ni^{2+} , H_3BO_3 and $\text{Al}(\text{NO}_3)_3 \cdot 9\text{H}_2\text{O}$ of 12 mM, 0.1 M and 1.2 mM, respectively, ($\text{Al}^{3+}/\text{Ni}^{2+} = 10$ mol%, $\text{Al}^{3+}/(\text{Al}^{3+} + \text{Ni}^{2+}) = 9$ mol%). Hundred to 300 cm³ of the Ni reaction solution were added in the polypropylene bottle containing 20 mg oxidized carbon. The mixture was shaken ultrasonically until carbon particles were completely dispersed. The bottle was then placed in a water bath at 50 °C for 48 h to form Ni–Al LDH-loaded carbon. The resulting Ni–Al LDH/C was collected by suction filtration, washed repeatedly with hot deionized water and dried at 50 °C for 3 h. The LDH content and $\text{Al}^{3+}/(\text{Ni}^{2+} + \text{Al}^{3+})$ for the Ni–Al LDH/C are defined as follows.

$$(\text{LDH content}/\text{wt}\%) = 100 \times m_{\text{LDH}}/(m_{\text{LDH}} + m_{\text{CB}}) \quad (5)$$

$$(\text{Al}^{3+}/(\text{Ni}^{2+} + \text{Al}^{3+}))/\text{mol}\% = 100 \times n_{\text{Al}^{3+}}/(n_{\text{Ni}^{2+}} + n_{\text{Al}^{3+}}) \quad (6)$$

where m_{LDH} , m_{CB} , $n_{\text{Al}^{3+}}$ and $n_{\text{Ni}^{2+}}$ are masses of LDH and carbon black and moles of Al^{3+} and Ni^{2+} , respectively. Their numerical values are summarized in Table 1.

2.2. Characterization

The concentrations of Ni^{2+} and Al^{3+} in the Ni–Al LDH/C composite or parent solution were determined by inductively coupled plasma-atomic emission spectroscopy (ICP-AES, HORIBA Ltd., ULTIMA 2000). Five milligrams of the composite were ultrasonically dispersed in 50 cm³ of diluted HNO_3 solution (0.26 M), and stored in the oven at 50 °C for 48 h to allow dissolution of Ni^{2+} and Al^{3+} . The dispersion was then filtrated to remove carbon, and the filtrate was used for the ICP-AES measurements. The crystalline structure of the composites was characterized using an X-ray diffractometer (Rigaku RINT-TTR/S2). The surface morphology was observed by field emission scanning electron microscope (JEOL JEM-6335F).

2.3. Electrode fabrication and performance

The positive electrode was fabricated as follows: 5 mg of the Ni–Al LDH/C composite was mixed with 20 mg of 2 g cm^{−3} polyvinyl alcohol (PVA) aqueous solution as a binder to make a paste. The resulting paste was loaded into a 1 × 1 cm² nickel foam, dried under vacuum at 80 °C for 1 h, then pressed at 20 MPa for 1 min using a programmed digital press (Shinto Digital Press, Japan). The negative electrode was constructed in a same way as the positive electrode. Hundred milligram of hydrogen storage alloy powder consisting of AB5-type rare earth-based mischmetal provided by

Table 1
Active materials specifications.

Samples No.	Total volume reaction solution (cm ³)	LDH content (wt%)	$\text{Al}^{3+}/(\text{Ni}^{2+} + \text{Al}^{3+})$ (mol%)
1	100	67.6	17.8
2	150	80.0	17.7
3	200	86.2	19.2
4	250	83.6	17.8
5	300	84.2	18.0

Kawasaki Heavy Industries, Akashi, Japan was mixed with $44.4 \times 10^{-6} \text{ dm}^3$ of PVA solution to make a paste. The paste was loaded into a $2 \times 1.5 \text{ cm}^2$ nickel foam, dried under vacuum at 120°C for 1 h, and pressed under 118 MPa for 60 s. The Hg/HgO into 6 M KOH was employed as the reference electrode while 6 M KOH solution served as an electrolyte solution. Charge–discharge measurements were performed using a potentiostat (HOKUTO DENKO HZ5000, Japan). Each cell was immersed into 6 M KOH at open circuit voltage for 3 days for conditionings, and the electrolyte solution was deaerated by argon bubbling for 15 min prior to measurements. It was then activated by charging and discharging at the 5.0 C-rate for 50 cycles. For the performance test, the activated cell was charged at 1.0 C-rate for 1.2 h and discharged to 0 mV vs. Hg/HgO. The durability test of the positive electrode containing 86.2 wt% LDH content and 19.2 mol% $\text{Al}^{3+}/(\text{Ni}^{2+} + \text{Al}^{3+})$ was evaluated by charging at 2.0 C-rate for 30 min and discharging at the same current to 0 V vs. Hg/HgO for 300 cycles under half cell conditions. Cyclic voltammetric measurements were carried out using a Solartron SI 1287 Electrochemical Instrument at a scan rate of 1 mV s^{-1} after charge–discharge tests.

3. Results and discussion

3.1. Effect of composition

In the LPD process, the term “reaction solution” designates the bulk solution containing reactants that interact with each other to promote deposition of metal oxide. Several parameters such as the reaction time, temperature and reactant concentrations are known to influence the deposition process [23]. By varying only the total volume of the reaction solution, it is possible to discover whether there is some relationship between the quantity of reactants and the amount of the deposited metal oxide. The variation of the LDH content and $\text{Al}^{3+}/(\text{Al}^{3+} + \text{Ni}^{2+})$ for the resultant composite as a function of the total volume of the reaction solution is plotted in Fig. 1. We can see that when the amount of carbon substrate is 20 mg and $\text{Al}^{3+}/\text{Ni}^{2+}$ of the reaction solution is 9 mol%, the amount of deposited Ni–Al LDH or LDH content increases with increasing the total volume up to 200 cm^3 , corresponding to a LDH content of 86.2 wt%. Thereafter it slightly decreases and remains almost constant at higher volumes, signifying that the amount of deposited Ni–Al LDH or LDH content does not essentially depend on the total volume of the reaction solution.

It is known that the deposition mechanism in the LPD process proceeds by a slow hydrolysis of an aqueous solution of a metal-

fluoro complex $[\text{MF}_x]^{(x-2n)-}$ with the addition of water, boric acid (H_3BO_3) and/or aluminum. The addition of water directly forces the precipitation of the oxide while boric acid and/or aluminum acts as the fluoride scavenger and destabilizes the fluoro-complex to force the oxide precipitation. This step allows a much better control of the hydrolysis reaction and of the solution's supersaturation. Once the solubility limit of oxide is reached, homogeneous nucleation occurs, and thin films of crystal and random structured oxide layer are formed on the substrate and grow up [22]. Oxidized carbon particles dispersed in the reaction solution possess curved surfaces and are subject to van der Waals forces and Brownian motion, while the influence of gravity can be negligible. The growth process depends on the geometry of the reaction field. Wilen and Polturak have demonstrated that the curvature of the surface plays an important role in the film growth near the saturation conditions [24]. In the present case, we assume that the film growth process is mainly influenced by the distance between each particle, which depends on the ratio between the amount of carbon (in mg) and the total volume of the reaction solution (in cm^3). Therefore, 20 mg of carbon versus 200 cm^3 of reaction solution appears to be the optimal composition that satisfies the saturation conditions.

It is noteworthy to mention that Raman spectroscopic studies (not shown) of the reaction solution without any substrate maintained under the same reaction conditions showed no change in the spectra, which leads to the conclusion that in the LPD process, the deposition occurs at the interface between the substrate and the bulk solution which constitutes the reaction zone. In other words, no deposition occurs without a substrate.

On the other hand, the $\text{Al}^{3+}/(\text{Al}^{3+} + \text{Ni}^{2+})$ did not significantly change when the total volume of the reaction solution increases from 100 to 300 cm^3 , although the $\text{Al}^{3+}/(\text{Al}^{3+} + \text{Ni}^{2+})$ increased by 8 mol% between 150 and 200 cm^3 , and decreased by the same mol% between 200 and 250 cm^3 . An approximately 25% increase in LDH content occurs between 100 and 200 cm^3 , which remains effectively constant thereafter. Since the Ni–Al stoichiometry is the same in all the solutions these results indicate that the $\text{Al}^{3+}/(\text{Al}^{3+} + \text{Ni}^{2+})$ also does not depend on the amount of deposition. Details regarding the mechanism of deposition of $\text{Ni}(\text{OH})_2$ as well as discussions on which one of the deposition and Al substitution occurs first in the reaction are far beyond the scope of this work. Fundamentals studies are on the process and these aspects will be elucidated in the future.

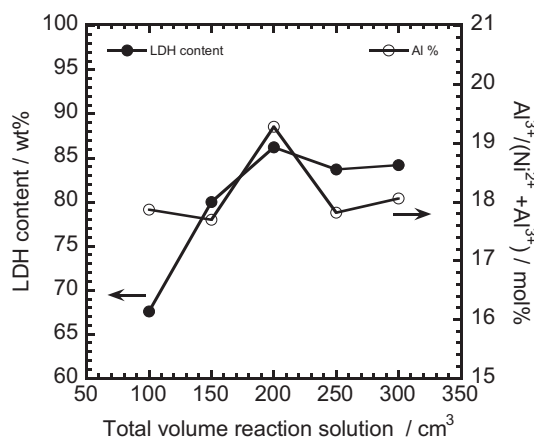


Fig. 1. Variation of $\text{Al}^{3+}/(\text{Al}^{3+} + \text{Ni}^{2+})$ ratio and LDH content as a function of the total volume of reaction solution.

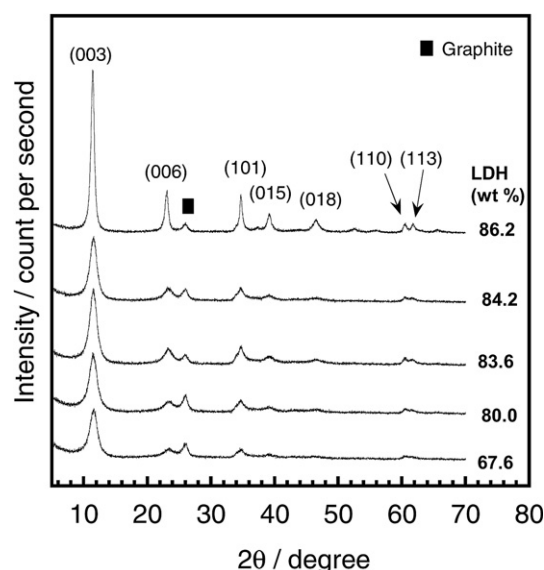


Fig. 2. XRD patterns of Ni–Al LDH/C with various LDH contents.

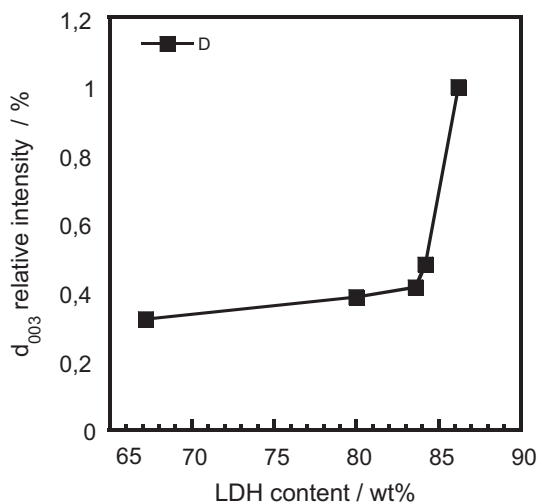


Fig. 3. Variation of the d_{003} relative intensity as a function of LDH content.

3.2. Diffraction studies

XRD patterns of the as-prepared Ni–Al LDH/C composites with various LDH contents are shown in Fig. 2. Obviously, all the samples exhibit the same diffraction characteristics of Ni–Al LDH [10,13,25], isostructural to α -Ni(OH) $_2$ ·0.75H $_2$ O (JCPDS card# 38-715). The peak intensities increase with increasing LDH content. The composite with the highest LDH content (86.2 wt%) shows narrow, sharp and more symmetrical peaks, indicative of a more ordered structure than other compositions. The relative intensity of the (003) reflection peak can be used to assess the degree of crystallinity of materials, the higher the intensity, the higher the crystallinity [10]. The variation of the (003) peak relative intensity as a function of LDH content is shown in Fig. 3. The relative intensity slowly increases with increasing LDH content up to 84.2 wt %. Then it abruptly increases until reaching its maximum at 86.2 wt%. In our previous work, we have observed that a higher crystallinity could be achieved for the sample containing 17.8 Al% [16]. In this work, using the same Ni–Al stoichiometry for the preparing sample with Al $^{3+}$ content of 17.8 Al%, we realize that the higher crystallinity can be achieved for the sample with 19.2 Al%, which corresponds to the highest LDH content. Finally, in regard with the improvement of the

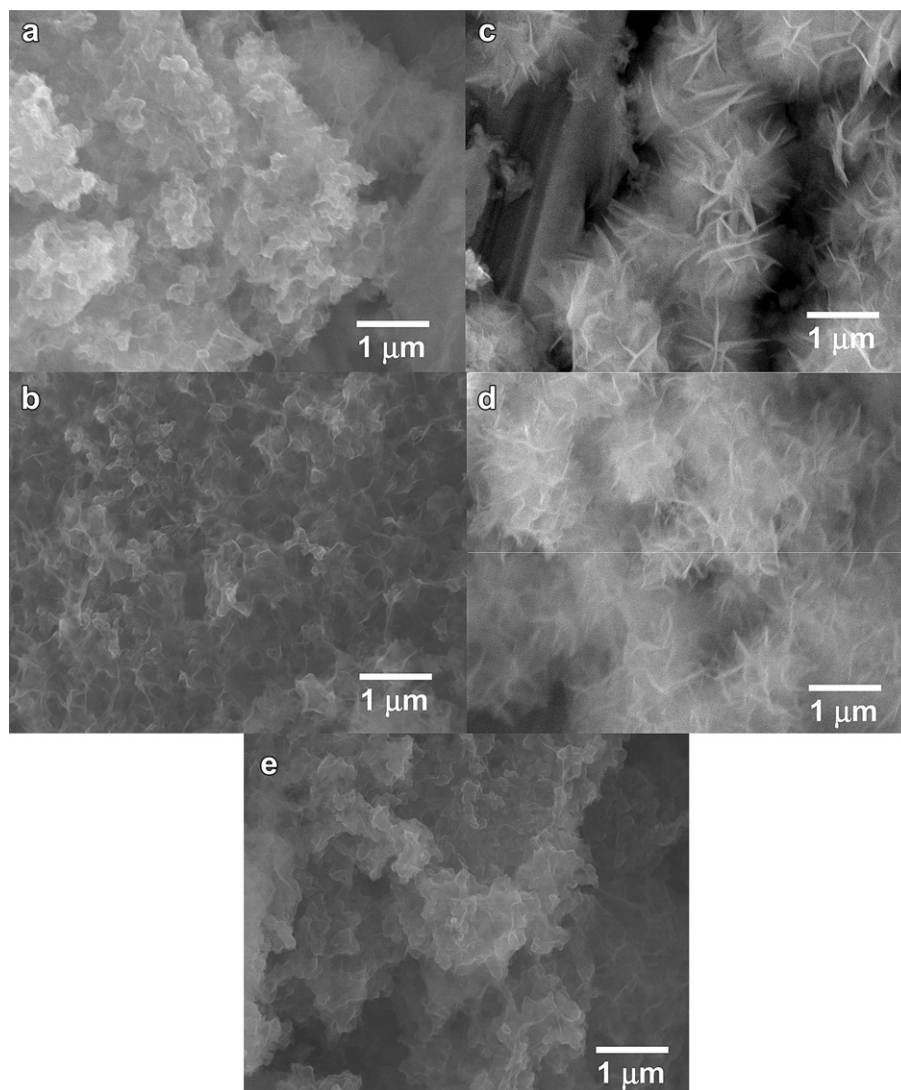


Fig. 4. Top view SEM images of Ni–Al LDH/C composites at various LDH contents: (a) 67.2 wt%, (b) 80.0 wt%, (c) 86 wt%, (d) 83.6 wt%, and (e) 84.2 wt%.

synthetic method for LDH, the compositional stoichiometry of 1:10 between carbon particles (in mg) and the total volume of reaction solution (in cm^3) can be considered as the optimal condition for achieving Ni–Al LDH/C composite with higher crystallinity.

3.3. Composition and morphologies

Fig. 4 illustrates the SEM micrographs of the as-prepared Ni–Al LDH/C composites for various total volumes of the reaction solution. Two characteristics can be distinguished: (i) samples with pronounced nickel matrix (Fig. 4(c) and (d)) and samples with pronounced carbon particles (Fig. 4(a), (b) and (e)). These images illustrate the disparity between the LDH content and the total volume of the reaction solution as discussed in the above section, and confirm that the composition of 20 mg carbon and 200 cm^3 reaction solution represents the optimal conditions for both deposition and film growth in this process. Features in Fig. 4(c) and (d) display the same characteristics of thin crumpled sheets without definite shape reported in our previous work [16], which are usually observed for turbostratic materials [25,26].

3.4. Charge–discharge performance

Charge–discharge curves (15th cycle) at 1.0 C-rate (2 mA) of electrodes containing Ni–Al LDH/C active materials with different LDH contents are shown in Fig. 5. It can be easily noticed that the electrode with 86.2 wt% LDH content and $\text{Al}^{3+}/(\text{Al}^{3+} + \text{Ni}^{2+})$ of 19.2% displays the best performance in this study. On its charge curve, a single flat plateau well separated from oxygen evolution indicates both a low polarization and a greatly reduced oxygen parasitic reaction. On its discharge curve, a single flat discharge plateau is observed between 380 and 320 mV vs. Hg/HgO. A discharge capacity of 393 $\text{mAh g}_{\text{comp}}^{-1}$ was obtained at 86.2 wt% LDH content, corresponding to 1.35 exchanged electrons per Ni atom in a gram of composite. A similar result was obtained by Li et al. [27] with 20.4 mol% Al-containing α -Ni(OH) $_2$ hollow spheres and Zhao et al. [28] with 19.5 mol% Al-substituted α -Ni(OH) $_2$ prepared by homogenous precipitation with urea. Hu et al. [29] and Wu et al. [30] obtained similar performance at 0.2 C-rate with their Al-stabilized α -Ni(OH) $_2$ prepared by a synthetic route assisted with hydrothermal treatment and by homogenous precipitation with urea, respectively. However, the former authors noticed that

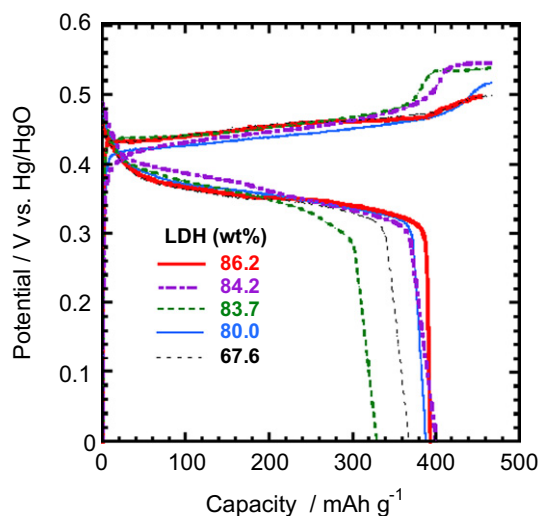


Fig. 5. Fifteenth charge–discharge curves at 1.0 C-rate (2 mA) of cathodes containing various LDH contents.

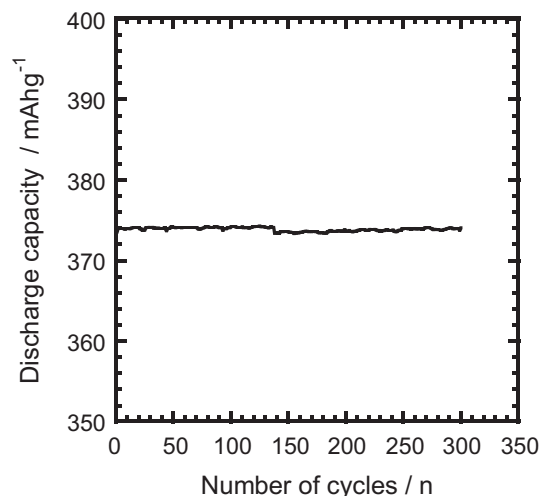


Fig. 6. Cycle life at 2.0 C-rate (5 mA) of the electrode containing 86.2 wt% LDH and 19.2 $\text{Al}^{3+}\%$ over 300 cycles.

a prolonged hydrothermal treatment led to formation of β -Ni(OH) $_2$. The evolution of the discharge capacity of the electrode with 86.2 wt% LDH content and 19.2 mol% $\text{Al}^{3+}/(\text{Al}^{3+} + \text{Ni}^{2+})$ as a function of the number of cycle is plotted in Fig. 6. The electrode presents a constant discharge capacity of ca. 372 $\text{mAh g}_{\text{comp}}^{-1}$ throughout 300 charge–discharge cycles without any fading. The higher capacity is attributed to the combination of the good crystallinity with the optimum $\text{Al}^{3+}/(\text{Al}^{3+} + \text{Ni}^{2+})$ in Ni(OH) $_2$ lattice which ensures a better chemical stability. These results are not only in good agreement with our previous findings [16] but they confirm that LPD-prepared LDH/C composites can be used as high rate electrode materials [31].

3.5. Cyclic voltammetry

Fig. 7 shows the cyclic voltammograms (10th cycle) of the electrode with 86.2 wt% LDH content and 19.2 Al mol% measured after 300 charge–discharge cycles. A unique redox couple with oxidation (anodic) peak prior the oxygen evolution, E_a at 464 mV and reduction (cathodic) peak, E_c at 309 mV on the reverse sweep is

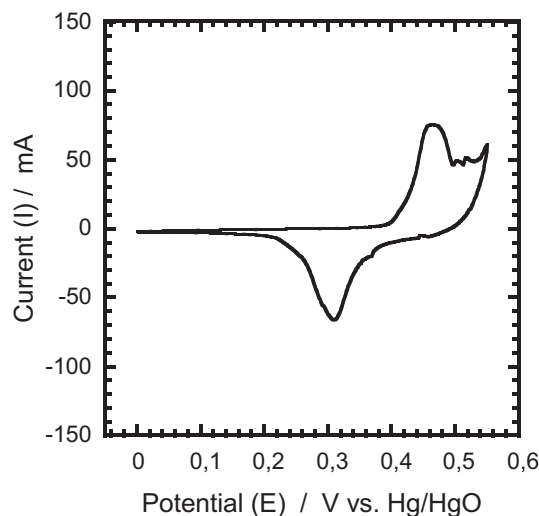


Fig. 7. Cyclic voltammogram of the electrode containing 86.2 wt% LDH and 19.2 $\text{Al}^{3+}\%$ at 1 mV s^{-1} .

observed. Relying on the uniqueness of the redox peaks and the chemical stability of our LPD-prepared Ni–Al LDH/C composites [16,17], we may assign these peaks to the γ -NiOOH/ α -Ni(OH)₂ reaction process. The potential difference between the anodic and cathodic peaks, $\Delta E_{a,c}$, is an important parameter to evaluate the electrochemical properties of an electrode. Generally, it is used to estimate the reversibility of the electrochemical redox reaction; the higher reversibility, the smaller $\Delta E_{a,c}$ [32]. The peak separation ($\Delta E_{a,c}$) of 155 mV is observed even after 300 cycles, suggesting that the γ -NiOOH/ α -Ni(OH)₂ reaction process is maintained over 300 cycles. These results undermine the electrochemical stability of the electrode containing Ni–Al LDH/C composite as active materials.

After evaluating the effects of the $\text{Al}^{3+}/(\text{Al}^{3+} + \text{Ni}^{2+})$ in our previous work [16], the present experiments have enabled us to establish an optimized synthetic route for high performance Ni–Al LDH/C active materials for use in the Ni cathodes. The application of these materials to Ni–MH cells is presently under study.

4. Conclusion

The effects of the LDH content on the structure and morphology of the composite are investigated. The sample prepared with 10 mol % $\text{Al}^{3+}/\text{Ni}^{2+}$ and 20 mg of carbon in 200 cm³ of reaction solution shows improved crystallinity, a higher LDH content (86.2 wt %) as well as an optimal $\text{Al}^{3+}/(\text{Al}^{3+} + \text{Ni}^{2+})$ (19.2 Al%). The resulting positive electrode showed promising electrochemical properties. A high performance is achieved at the 1.0 C-rate with a discharge capacity of 393 mAh g_{comp}^{−1} which corresponds to 1.35 exchanged electrons of per Ni atom. The electrode also displays excellent capacity retention over 300 charge–discharge cycles at the 2.0 C-rate, suggesting that LPD-prepared Ni–Al LDH/C can be used as high rate electrode materials. Cyclic voltammetry after 300 charge–discharge cycles confirms that the electrode possesses an excellent electrochemical stability. With further investigations on their electrochemical properties, Ni–Al LDH/C composites are expected to be applied in the next generation of Ni–MH secondary batteries.

Acknowledgments

This study was carried out as the Energy and Environment Technologies Development Projects; “Development of an Electric Energy Storage System for Grid-connection with New Energy Resources” supported by Kawasaki Heavy Industries Ltd. and New Energy and Industrial Technology Organization (NEDO), and Grant-in-Aid for Scientific Research (B) No. 22350094, JSPS, Japan

(KAKENHI). We are thankful to Ms. Hazuki Otsuka of Osaka Prefecture University for kind assistance during the experimental evaluation of the electrodes.

References

- [1] V.R. Allman, *Chimia* 24 (1970) 99–108.
- [2] M. Intissar, R. Segni, C. Payen, J.P. Besse, F. Leroux, *J. Solid State Chem.* 167 (2002) 508–517.
- [3] A.A. Bhattacharyya, G.M. Woltermann, J.S. Yoo, J.A. Karch, W.E. Cormier, *Ind. Eng. Chem. Res.* 27 (1988) 1456–1460.
- [4] A. Nakahira, T. Kubo, H. Murase, *IEEE Trans. Magn.* 43 (2007) 2442–2444.
- [5] S.V. Prasanna, P.V. Kamath, C. Shivakumara, *Mater. Res. Bull.* 42 (2007) 1028–1039.
- [6] D. Tichit, M.J. Ortiz, D. Francova, C. Gérardin, B. Coq, R. Durand, F. Prinetto, G. Ghiotti, *Appl. Catal. A: Gen.* 318 (2007) 170–177.
- [7] M. Taibi, S. Ammar, N. Jouini, F. Fiévet, P. Molinié, M. Drillon, *J. Mater. Chem.* 12 (2002) 3238–3244.
- [8] A. Nakahira, H. Murase, *J. Appl. Phys.* 101 (2007) 09N516-3.
- [9] P.V. Kamath, G.H.A. Therese, *J. Solid State Chem.* 128 (1997) 38–41.
- [10] A. Sugimoto, S. Ishida, K. Hanawa, *J. Electrochem. Soc.* 146 (1999) 1251–1255.
- [11] P.V. Kamath, M. Dixit, L. Indira, A.K. Shukla, V.G. Kumar, N. Munichandraiah, *J. Electrochem. Soc.* 141 (1994) 2956–2959.
- [12] H. Chen, J.M. Wang, Y.L. Zhao, J.Q. Zhang, *J. Solid State Electrochem.* 9 (2005) 421–428.
- [13] W.K. Hu, D. Noréus, *Chem. Mater.* 15 (2003) 974–978.
- [14] L.J. Yang, X.P. Gao, Q.D. Wu, H.Y. Zhu, G.L. Pan, *J. Phys. Chem. C* 111 (2007) 4614–4619.
- [15] F. Yang, B.Y. Xie, J.Z. Sun, J.K. Jin, M. Wang, *Mater. Lett.* 62 (2008) 1302–1304.
- [16] A.B. Béléké, M. Mizuhata, *J. Power Sources* 195 (2010) 7669–7676.
- [17] M. Mizuhata, A. Hosokawa, A.B. Béléké, Shigehito Deki, *ECS Trans.* 19 (2009) 41–46.
- [18] H. Nagayama, H. Honda, H. Kawahara, *J. Electrochem. Soc.* 135 (1988) 2012–2016.
- [19] S. Deki, H. Niu Yu Yu Ko, T. Fujita, K. Akamatsu, M. Mizuhata, A. Kajinami, *Eur. Phys. J. D* 16 (2001) 325–328.
- [20] S. Deki, S. Iizuka, A. Horie, M. Mizuhata, A. Kajinami, *Chem. Mater.* 16 (2004) 1747–1750.
- [21] S. Deki, S. Iizuka, K. Akamatsu, M. Mizuhata, A. Kajinami, *J. Am. Ceram. Soc.* 88 (2005) 731–736.
- [22] S. Deki, A. Hosokawa, A.B. Béléké, M. Mizuhata, *Thin Films Solids* 517 (2009) 1546–1554.
- [23] P. Oliva, J. Leonardi, D. Delmas, J.J. Braconnier, M. Figlarz, F. Fievet, A. de Guibert, *J. Power Sources* 8 (1982) 229–255.
- [24] L. Wilen, E. Polturak, *Phys. Rev. A* 41 (1990) 6838–6844.
- [25] Y. Li, X. Xie, J. Liu, M. Cai, J. Rogers, W. Shen, *Chem. Eng. J.* 136 (2008) 398–408.
- [26] L. Lei, M. Hu, X. Gao, Y. Sun, *Electrochim. Acta* 54 (2008) 671–676.
- [27] Y. Li, W. Li, S. Chou, J. Chen, *J. Alloys Compd.* 456 (2008) 339–343.
- [28] Y.L. Zhao, J.M. Wang, H. Chen, T. Pan, J.Q. Zhang, C.N. Cao, *Int. J. Hydrogen Energy* 29 (2004) 889–896.
- [29] W.K. Hu, X.P. Gao, D. Noréus, T. Burchardt, N.K. Nakstad, *J. Power Sources* 8 (1982) 229–255.
- [30] Q.D. Wu, X.P. Gao, G.R. Li, G.L. Pan, T.Y. Yan, H.Y. Zhu, *J. Phys. Chem. C* 111 (2007) 17082–17087.
- [31] B. Liu, Z. Yunshi, H. Yuan, H. Yang, E. Yang, *Int. J. Hydrogen Energy* 25 (2000) 333–337.
- [32] D.A. Corrigan, R. M Bendert, *J. Electrochem. Soc.* 136 (1989) 723–728.